



**HAL**  
open science

## Using the Distribution of Relaxation Times for analyzing the Kramers-Kronig Relations in Electrochemical Impedance Spectroscopy

Bernhard Zeimetz, Aurelien Flura, Jean-Claude Grenier, Fabrice Mauvy

► **To cite this version:**

Bernhard Zeimetz, Aurelien Flura, Jean-Claude Grenier, Fabrice Mauvy. Using the Distribution of Relaxation Times for analyzing the Kramers-Kronig Relations in Electrochemical Impedance Spectroscopy. 2018. hal-01692003v1

**HAL Id: hal-01692003**

**<https://hal.science/hal-01692003v1>**

Preprint submitted on 24 Jan 2018 (v1), last revised 21 Feb 2018 (v2)

**HAL** is a multi-disciplinary open access archive for the deposit and dissemination of scientific research documents, whether they are published or not. The documents may come from teaching and research institutions in France or abroad, or from public or private research centers.

L'archive ouverte pluridisciplinaire **HAL**, est destinée au dépôt et à la diffusion de documents scientifiques de niveau recherche, publiés ou non, émanant des établissements d'enseignement et de recherche français ou étrangers, des laboratoires publics ou privés.

*Submitted to Electrochimica Acta (January 2018)*

## **Using the Distribution of Relaxation Times for analyzing the Kramers-Kronig Relations in Electrochemical Impedance Spectroscopy**

Bernhard Zeimetz\*, Aurélien Flura, Jean-Claude Grenier, Fabrice Mauvy

Institute for Condensed Matter Chemistry Bordeaux, ICMCB, CNRS, Université Bordeaux,  
87 Av. Dr Schweitzer, 33608 PESSAC, France

\*corresponding author: [bernhard.zeimetz@cnrs.fr](mailto:bernhard.zeimetz@cnrs.fr)

### **Keywords**

Electrochemical Impedance Spectroscopy; Distribution of Relaxation Times; Kramers-Kronig Relations; Data Integrity

### **Abstract**

We propose to verify the Kramers-Kronig Relations (KKR) through comparison of two versions of the Distribution of Relaxation Times (DRT), calculated from the real and imaginary part of the impedance.

When checking the integrity of impedance spectroscopy data, this method is useful to interpret correctly results when a direct calculation of the KKR integrals shows a deviation from measured data. Our method can distinguish cases (i) where a deviation from the KKR indicates genuine physical problems during the measurement from (ii) a deviation arising when the frequency range accessible by the measurement is insufficiently large.

## 1 Introduction

Electrochemical Impedance Spectroscopy [1] (EIS) is commonly used to identify the various characteristics of an electrochemical system, as for instance electrode phenomena in fuel cells. The method consists in measuring the complex impedance  $Z = Z' + iZ''$  as a function of AC frequency. The data are then usually fitted to a system model based on a so-called electrical equivalent circuit, each element of the circuit representing a physical characteristic of the studied system. The main difficulty is the prior choice of the equivalent circuit (numbers of elements, impedance form) that can reliably represent the physical phenomena.

Often, EIS measurements are carried out at very high temperatures, sometimes in strongly corrosive environments, or other extreme conditions. Hence, a specific difficulty of EIS experiments is the stability of the sample, temperature and other conditions during a measurement, which can last between some minutes and some hours. Testing the integrity of measured data is therefore a crucial part of the analysis.

### 1.1 Kramers-Kronig Relations

The Kramers-Kronig Relations (KKR) between the real and imaginary part of the electrical impedance  $Z = Z' + i Z''$  are defined as

$$(1a) \quad Z'(\omega) = R_0 + 2 \omega / \pi \int_0^{\infty} (x/\omega Z''(x) - Z''(\omega)) / (x^2 - \omega^2) dx$$

$$(1b) \quad Z''(\omega) = 2 \omega / \pi \int_0^{\infty} (x/\omega Z'(x) - Z'(\omega)) / (x^2 - \omega^2) dx$$

where  $\omega = 2 \pi f$  is the radial frequency and  $R_0$  is the DC resistance.

The KKR are used as a check of data integrity in impedance spectroscopy [2-4], by plotting the measured data  $Z'$  and  $Z''$  against those calculated from the integrals. Of course, full precision cannot be attained because infinite frequency as in the integral is not accessible. However, the direct calculation of the KKR integral yields an approximately correct result if the measured frequency range is sufficiently large, in the sense that semi-circles or semi-arcs in the Nyquist plot ( $Z'$  vs  $Z''$ ) are completed.

If this is not the case, and semi-arcs are not completed, the direct calculation of the KKR yields a deviation, which is difficult to distinguish from deviations with an intrinsic physical origin (examples are shown below, Figs 2 and 3). Extrapolation of the data has been proposed [3] as a possible solution, but such an extrapolation is always based on selection of a physical model, and thereby on an implicit assumption of data integrity.

## 1.2 Distribution of Relaxation Times

The Distribution of Relaxation Times (DRT)  $G(\tau)$  is another much-used quantity for interpreting measurement data [5-9]. It is related to the impedance via the following equations:

$$(2a) \quad Z'(\omega) = R_0 \int_0^{\infty} (G(\tau) / (1 + \omega^2 \tau^2)) d\tau$$

$$(2b) \quad Z''(\omega) = R_0 \int_0^{\infty} (\omega \tau G(\tau) / (1 + \omega^2 \tau^2)) d\tau$$

or in complex form

$$(3) \quad Z(\omega) = R_0 \int_0^{\infty} (G(\tau) / (1 + i \omega \tau)) d\tau$$

Hence one can calculate the DRT  $G(\tau)$  from either the real part  $Z'$  or the imaginary part  $Z''$  of the impedance. By plotting the DRT instead of measured data  $Z$ , one can often identify more clearly different time constants contributing to the overall impedance of a composite system [9]. The DRT analysis thereby helps to identify an equivalent circuit that can be subsequently used to fit the  $Z$  data.

The basis of the DRT formalism is the representation of  $Z$  as a (finite or infinite) series of R-C elements (each with R parallel C), using  $Z_{RC} = R/(1 + i \omega \tau)$ ,  $\tau = RC$  and  $G(\tau)$  as a weighting function. This implies an important limitation of the DRT method: an impedance including inductive components cannot be represented as described above [2,9]. Such inductive signals are typically generated in EIS measurements by wiring at high frequencies.

For the purpose of this work, we emphasize that for a given impedance  $Z = Z' + i Z''$ , the DRT function  $G(\tau)$  in (2a), (2b) and (3) is, in theory, identical.

### 1.3 Connecting Kramers-Kronig Relations and Distribution of Relaxation Time

The similar form of the equations (1a-b) and (2a-b) suggests that they are related. And indeed, it was shown many years ago [10] that if two functions  $Z'$  and  $Z''$  are constructed from a single DRT via equations (2a) and (2b), they fulfill the KKR.

We conclude that conversely, if the two DRTs calculated from measured impedance components  $Z'$  and  $Z''$  are identical, we can conclude that  $Z'$  and  $Z''$  fulfill the KKR. We show in this work that this relationship can be used to test the KKR more reliably, compared to a direct integration.

In the following, we will denote the DRTs calculated from  $Z'$  and  $Z''$  as  $G_{Re}$  and  $G_{Im}$ , respectively.

## 2 Experimental and Computational Methods

### 2.1 Computer simulations and numerical methods

(Figure 1)

Synthetic impedance data  $Z = Z' + i Z''$  were produced with the circuit simulation program *ngspice* [11]. Fig. 1 shows the circuit and parameters used for this work. The basic circuit element consisted of a resistor in parallel to a capacitor. For the reference circuit, labelled A, three such R-C elements were placed in series, with an additional offset  $R_0$ .

An outstanding feature of *ngspice* is the possibility to add user-defined circuit elements. In order to mimic a measurement with drifting resistance offset, we added a frequency-dependent resistance  $R_4$  in one simulation, labelled C below.

DRTs from both synthetic and experimental impedance data were calculated using the software *DRTtools* [12]. The programme uses Tikhonov regularization and offers to the user choice of a number of numerical parameters. The selection of these parameters for this work is discussed in detail in the Appendix. While *DRTtools* provides the output data in the form  $G(\tau)$  as in eq. 2, we

display the DRT data in this work as function of decimal logarithm of frequency  $f = 1/(2 \pi \tau)$ , which facilitates direct comparison with impedance data.

A crucial feature of *DRTtools* for our work is the ability to calculate from real and imaginary parts of the impedance two separate DRTs,  $G_{Re}$  and  $G_{Im}$ .

Another feature of *DRTtools* is the extrapolation of DRT data beyond the frequency range  $f_{min}$ ,  $f_{max}$  of the input data. This is problematic as it can lead to spurious peaks or shoulders, as discussed below.

As a quantitative test for comparing the two curves  $G_{Re}$  and  $G_{Im}$  we employed a variation of the coefficient of determination  $r^2$  [13]

$$(4) \quad r^2 = 1 - \sum_i (G_{re}(i) - G_{im}(i))^2 / \sum_i (G_{re}(i) - \bar{G}_{re})^2 ,$$

where  $\bar{G}_{re}$  is the mean value of  $G_{re}$ .  $r^2$  values close to 1 indicate near-perfect overlap of data sets. The data range for calculating  $r^2$  was limited to the input frequency range, that is extrapolated data of  $G$  where not included, for reasons explained above.

In order to test the Kramers-Kronig relations, the integrals in equations 1a and 1b were calculated numerically in a home-made program, by first applying to the data a cubic spline fit [14] and then summing over the function values. The singularity in Eq. 1 was treated as described in Ref. [3].

## 2.2 Experimental data

Data analysis with calculation of Kramers-Kronig integrals and DRTs was also applied to experimental data from three different symmetric half-cells. The component materials of the cells, and EIS measurement temperatures are summarised in Table 1.

Two materials were used for the preparation of the dense electrolytes: powder of GDC ( $Ce_{0.8}Gd_{0.2}O_{1.90}$ ) was purchased from Marion Technologies comp., and shaped to discs of roughly 18.5 mm diameter, thickness 1 mm and relative density > 95% after pressing the powder in a die, followed by a sintering step at 1500°C for 3h. Dense Ø25 mm, 90 µm thick ceramic discs of TZ3Y (3 mol.%  $Y_2O_3-ZrO_2$ ) were purchased from Indec Company.

For TZ3Y electrolytes (samples E and F), PrDC ( $\text{Ce}_{0.7}\text{Pr}_{0.3}\text{O}_{2-\delta}$ , Praxair) was used as barrier interlayer between the electrode and the electrolyte. It was screen-printed on TZ3Y and sintered at 1300 °C for 3h in air, with a controlled heating rate of 2 °C/min, resulting in a layer thickness of roughly 3  $\mu\text{m}$ .

The electrodes powder LNO ( $\text{La}_2\text{NiO}_{4+\delta}$ ) and PNO ( $\text{Pr}_2\text{NiO}_{4+\delta}$ ) were purchased from Marion Technologies. They were screen-printed on top of PrDC or GDC and sintered in air at 1150 °C, 1h for PNO, and at 1200 °C, 1h for LNO, with a heating rate of 2 °C/min, resulting in an electrode layer of around 20  $\mu\text{m}$ .

An additional layer of LNF ( $\text{LaNi}_{0.6}\text{Fe}_{0.4}\text{O}_3$ ) was screen printed on top of LNO or PNO electrodes for samples D and F, in order to improve the overall current collection. It was *in-situ* sintered in the EIS setup at 900 °C for 2h.

Sample name	D	E	F
electrolyte	GDC	TZ3Y	TZ3Y
interlayer	-	PrDC	PrDC
electrode	PNO	PNO	LNO
collecting layer	LNF	-	LNF
EIS Measurement temperature	650 °C	550 °C	700 °C

*Table 1: Half-cell composition and measurement temperatures of selected data sets used for data analysis. See text for exact chemical compositions and other details.*

The setup used to perform electrochemical impedance spectroscopy (EIS) measurement has been described in detail by Flura *et al* [15]. Gold grids were used as current collectors. The electrochemical experiments were performed from 800 °C down to 500 °C, in air, at  $i_{\text{dc}} = 0$  A. Impedance measurements were carried out with an ac amplitude being fixed at 50 mV in the range 10<sup>5</sup> Hz - 10<sup>-1</sup> Hz using an Autolab® PGStat 302 frequency response analyser. Data at highest frequencies (10<sup>5</sup> – 10<sup>6</sup> Hz) were not considered due to experimental limitations (low value of the sample resistance, connection wires, impedance-meter characteristics).

### 3 Results and Discussion

We first demonstrate our method on synthetic, noise-free data. By using computer simulations, we can control the cause of deviations in the KK data, thereby directly testing our main hypothesis. We then move to experimental data from SOFC half-cells. Note that the data  $G_{Re}$ ,  $G_{Im}$  shown in this section have *not* been rescaled.

#### 3.1 Synthetic data

The simulated data shown in Fig. 2 are based on the simple circuit model detailed in Fig. 1. Sample A is the reference with 3 R-C elements, and an offset resistance  $R_0$ . Sample B is identical to A except that part of the data at lowest and highest frequencies were removed. For sample C, an additional 'drift' of the resistance was added.

(Figure 2)

Sample A in Fig. 2 demonstrates an ideal case where the Nyquist plot shows well-completed arcs  $Z'$  vs  $Z''$ . Here the direct calculation of KKR (red line) via numerical integration (Eq. 1) shows perfect alignment with 'measured' data. The two versions of the DRT,  $G_{Re}$  and  $G_{Im}$ , are identical as expected ( $r^2 \sim 1$  indicates near-perfect overlap of DRT curves.).

Sample B in Fig. 2 shows impedance data identical to example A except that the data at lowest and highest frequencies were removed. As a result of the removal of data, the two outer arcs in the Nyquist plot are not completed (note that in all the Nyquist plots of Fig. 2, the y-axis is scaled from 0 to 1.2 Ohms). As expected, the KKR calculation according to the integral Eq. 1 shows a deviation from the measured data (red line vs. points). However, the two DRT curves calculated from  $Z'$  and  $Z''$  are nearly identical. The difference at low frequencies occurs mainly outside of the range of input data, which is indicated by dotted lines. The discrepancy can be

attributed to the numerical extrapolation of DRT data, which adds spurious widening of the peak in  $G_{Re}$ .

Sample C, with a drifting  $R_4$  added, also shows deviation of KKR integration from the impedance data in the Nyquist plot. But here, also the two DRT curves are different:  $G_{Im}$  shows not only higher main peaks compared to  $G_{Re}$ , but also two additional smaller peaks, within the range of input data. We conclude that in this case the KKR deviation has a genuine 'physical' origin, which was of course built-in as part of the simulation.

Comparison of the Nyquist plots A and B shows that we can create a deviation of the KKR curve simply by removing part of the data. Comparison of samples B and C shows that a deviation of the KKR curve can look quite similar, even if the cause, insufficient data range or drifting resistance during measurement, is very different.

The DRT calculations support our main hypothesis: misinterpretation of the KKR data can be avoided by comparing the DRTs calculated from  $Z'$  and  $Z''$ : if  $G_{Re}$  and  $G_{Im}$  are (nearly) identical as in sample B, we can conclude that the KK deviation is due to an insufficient data range. In contrast the DRTs are significantly different as in sample C, the deviation of the KK data corresponds to a real instability or other problem in the measurement, as discussed in the introduction.

### 3.2 Experimental data

(Figure 3)

Sample D in Fig. 3 is an example where the Nyquist plot shows well-completed arcs  $Z'$  vs.  $Z''$ . The direct calculation of KKR (red line) via numerical integration (Eq. 1) shows very good alignment with measured data. On the right-hand side, the two versions of the DRT,  $G_{Re}$  and  $G_{Im}$ , are nearly identical. The differences at low frequencies can again be attributed to numerical effects via extrapolation.

Fig. 3, for sample E, experimentally measured data with the arcs in the Nyquist plot are not completed. As expected, the KKR calculation according to the integral Eq. 1 shows a deviation from the measured data (red line vs. points). However, the two DRT curves for sample E, calculated from  $Z'$  and  $Z''$ , are nearly identical ( $r^2 = 0.989$ ) within the frequency range of the input data, indicated by vertical dotted lines. Once again, the difference at low frequencies, outside of the range of input data, can be considered as a numerical artefact due to extrapolation.

We conclude that the apparent deviation of the KK integral is a purely mathematical effect caused by insufficient frequency range, and is not related to problems in the sample or measurement equipment.

Finally, for sample F (Fig. 3) exhibiting another kind of data, we can observe deviations in the KK curve, both at low and high frequencies. The DRT curves  $G_{Re}$  and  $G_{Im}$  are also different, both at low and high frequencies, and notably *inside* the measured frequency range. We thus conclude that in this case the KKR deviation is due to instabilities or other problems in the measurement. Indeed, we found that the sample showed fissures, indicating possible thermo-mechanical instability.

#### **4. Conclusions**

We have shown that, by calculating two DRT curves separately from the real and imaginary part of the impedance, we can determine whether the impedance data fulfill the Kramers-Kronig Relations (KKR). This method allows us to interpret correctly a direct KKR calculation via numerical integration, because it makes possible to distinguish cases where the KKR integral deviates due to physical origins, such as damaged samples, temperature drift, etc., from those cases when the deviation has a mathematical origin, caused by insufficient frequency range of measured impedance.

Our work also shows that extrapolating the DRT data beyond the measured frequency range is not always beneficial, as it can sometimes add spurious signals and thereby hinder correct analysis.

Finally, while KKR and DRT are two very popular methods for analyzing data in modern impedance spectroscopy, the connection between the two, although known since 1954 [10], has found little interest [16]. We believe that the relation between KKR and DRT, combined with modern numerical methods, has the potential to lead to other useful results, beyond the very specific use proposed in this work. We will explore this possibility in future work.

## **5. Acknowledgements**

This work made extensive use of several numerical software packages available on the World Wide Web (for details see section Computational Methods and References). We are grateful to the authors of the software for making their work available free of charge.

We thank Dr. Thomas Voisin for help with data analysis.

This research did not receive any specific grant from funding agencies in the public, commercial, or not-for-profit sectors.

## **Appendix: Selection of Modelling Parameters for calculation of DRTs**

The computer program DRTtools by Wan *et al.* [12] implements calculation of DRTs by Tikhonov regularization. The user can select a number of parameters for the calculation. Notably, one can choose as the data source either the real part of impedance, the imaginary part, or both combined. The main interest of the current paper is comparison of the results from real and imaginary parts. Wan *et al.* [12] have described in great detail the influence of the different parameters. Ivers-Tiffée *et al.* [9] focused on the regularization parameter  $\lambda$ , and investigated the influence of noise. For the present work, we decided to fix the parameters at given values, as follows:

Discretization method:     Gaussian Functions

Regularization parameter:  $\lambda = 0.1$

Regularization derivative: first order

Type of shape control:     Shape Factor

Shape Factor:                 $\mu = 0.88$

This choice of parameters was guided by the following observations:

1) As we wish to compare different calculations, we are interested not only in the position of the peaks, but in their height and shape. The results should also be rather insensitive to noise, and independent of the density of data points (number of points per frequency interval). The parameters cited above fulfill these conditions, even though they lead to rather broad peaks and thus low resolution.

2) Decreasing the value for  $\lambda$ , and changing 'type of shape control' results in narrower peaks, increasing the resolution. However, especially in the presence of noise, one often obtains spurious peaks [9], which would obscure the main findings of the present paper. Furthermore, the height of the peaks then depend on the density of the data. All this indicates that the DRT peak shapes are dominated by numerical effects when  $\lambda$  is too small.

3) As proposed by Wan *et al.* [12], we used the Havriliak Negami (HN) model [17] in order to check the validity of our calculations. The DRT for the HN model is known analytically [18], and we confirmed that our calculations of DRTs are indeed correct up to a scaling factor, as shown in Fig. 4.

(Figure 4)

(Figure 5)

4) The DRTs  $G_{Re}$  and  $G_{im}$  can also be calculated via Fourier Transforms (FT), after transforming equations (2a-b) into convolution integrals [5,6]. Fig. 5 shows a comparison of the two methods for the case of  $G_{Re}$ . In our opinion, the FT method is preferable in principle, because no additional numerical parameters, as compared to those above, have to be introduced, unless strong noise has to be smoothed (*cf.* the discussion in Ref.s [8] and [9]). Note that our data from FT

calculation in Fig. 5 were *not* post-treated with filters, as our data did not show oscillations as reported by other authors [6,7]. The selection of parameters for the Tikhonov method was guided by the objective to reproduce DRTs from the FT method at least approximately, as shown in Fig 5.

5) On the other hand, our preliminary attempts to implement the FT method was showing reasonable results only when  $Z'$  is used as data source, and calculation from  $Z''$  yielded spurious results for  $G_{lm}$ , even for noise-free, synthetic source data. The 'ill-posedness' of the convolution integral, and resulting instability of the solution against noise, is often cited [9,12] as a reason to prefer the regularization method, but our results indicate that this point requires further investigations.

## **References**

[1] A. Lasia, Electrochemical impedance spectroscopy and its applications, Springer New York 2014

<https://doi.org/10.1007/978-1-4614-8933-7>

[2] J. R. MacDonald and M. K. Brachman, Linear-System Integral Transform Relations, Rev. Mod. Phys. 28 (1956) 393

<https://doi.org/10.1103/RevModPhys.28.393>

[3] B. A. Boucamp, Practical Application of the Kramers-Kronig Transformation on Impedance Measurements in Solid State Electrochemistry, Solid State Ionics 62 (1993) 131

[https://doi.org/10.1016/0167-2738\(93\)90261-Z](https://doi.org/10.1016/0167-2738(93)90261-Z)

[4] M. E. Orazem, B. Tribollet, An Integrated Approach to Electrochemical Impedance Spectroscopy, Electrochimica Acta 53 (2008) 7360

<https://doi.org/10.1016/j.electacta.2007.10.075>

- [5] R. M. Fuoss and J.G. Kirkwood, Electrical Properties of Solids. VIII. Dipole Moments in Polyvinyl Chloride-Diphenyl Systems, J. Am. Chem. Soc. 63 (1941) 385  
<http://dx.doi.org/10.1021/ja01847a013>
- [6] A. D. Franklin, H. D. de Bruin, The Fourier Analysis of Impedance Spectra for Electroded Solid Electrolytes, Phys. Stat. Sol. 75 (1983) 647  
<http://dx.doi.org/10.1002/pssa.2210750240>
- [7] B. A. Boukamp, Fourier Transform Distribution Function of Relaxation Times; Application and Limitations, Electrochimica Acta 154 (2015) 35  
<https://doi.org/10.1016/j.electacta.2014.12.059>
- [8] B. A. Boukamp, Derivation of a Distribution Function of Relaxation Times for the (fractal) Finite Length Warburg, Electrochimica Acta 252 (2017) 154  
<https://doi.org/10.1016/j.electacta.2017.08.154>
- [9] E Ivers-Tiffée, A Weber, Evaluation of Electrochemical Impedance Spectra by the Distribution of Relaxation Times, Journal of the Ceramic Society of Japan 125 (2017) 193  
<https://doi.org/10.2109/jcersj2.16267>
- [10] M. K. Brachman, J. R. MacDonald, Relaxation-Time Distribution Functions and the Kramers-Kronig Relations, Physica 20 (1954) 266  
[https://doi.org/10.1016/S0031-8914\(54\)80271-0](https://doi.org/10.1016/S0031-8914(54)80271-0)
- [11] Software and manual available at <http://ngspice.sourceforge.net> (22/1/2018)
- [12] T. H. Wan, M. Saccoccio, C. Chen, F. Ciucci, Influence of the Discretization Methods on the Distribution of Relaxation Times Deconvolution: Implementing Radial Basis Functions with DRTtools, Electrochimica Acta, 184 (2015) 483-499.  
<http://dx.doi.org/10.1016/j.electacta.2015.09.097>
- Software available for download at <https://sites.google.com/site/drttools/> (22/1/2018)

- [13] W. M. Mendenhall, T. L. Sincich, Statistics for Engineering and the Sciences, 6th Ed., CRC Press 2016
- [14] C++ library for spline fits available at <https://www.eol.ucar.edu/software/bspline-c-template-library> (22/1/2018)
- [15] A. Flura, C. Nicollet, S. Fourcade, V. Vibhu, A. Rougier, J.-M. Bassat, J.-C. Grenier, Identification and Modelling of the Oxygen Gas Diffusion Impedance in SOFC Porous Electrodes: Application to Pr<sub>2</sub>NiO<sub>4+d</sub>, Electrochimica Acta, 174 (2015) 1030  
<http://dx.doi.org/10.1016/j.electacta.2015.06.084>
- [16] C. J. Dias, A Kramers-Kronig Integral Relation Turned into a Simple Convolution Operation and its Application to Dielectric Measurements, Applied Phys. Lett 103 (2013) 222903  
<https://doi.org/10.1063/1.4834315>
- [17] S. Havriliak, Jr., S. Negami, A Complex Plane Representation of Dielectric and Mechanical Relaxation Processes in some Polymers, Polymer 8 (1967) 161  
[https://doi.org/10.1016/0032-3861\(67\)90021-3](https://doi.org/10.1016/0032-3861(67)90021-3)
- [18] A. Bello, E. Laredo, M. Grimeau, Distribution of Relaxation Times from Dielectric Spectroscopy using Monte Carlo Simulated Annealing: Application to a-PVDF ,Phys Rev. B 60 (1997) 12764  
<https://doi.org/10.1103/PhysRevB.60.12764>

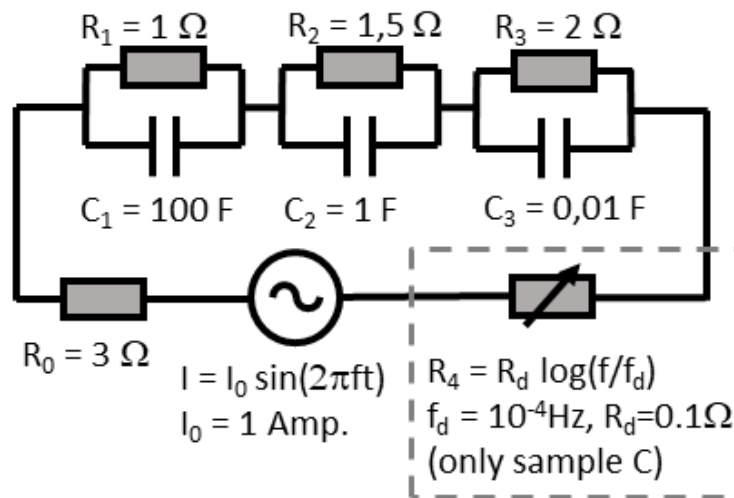


Fig. 1 Schematics and parameters used in circuit simulations for samples A, B, C, impedance and DRT data shown in Fig. 2

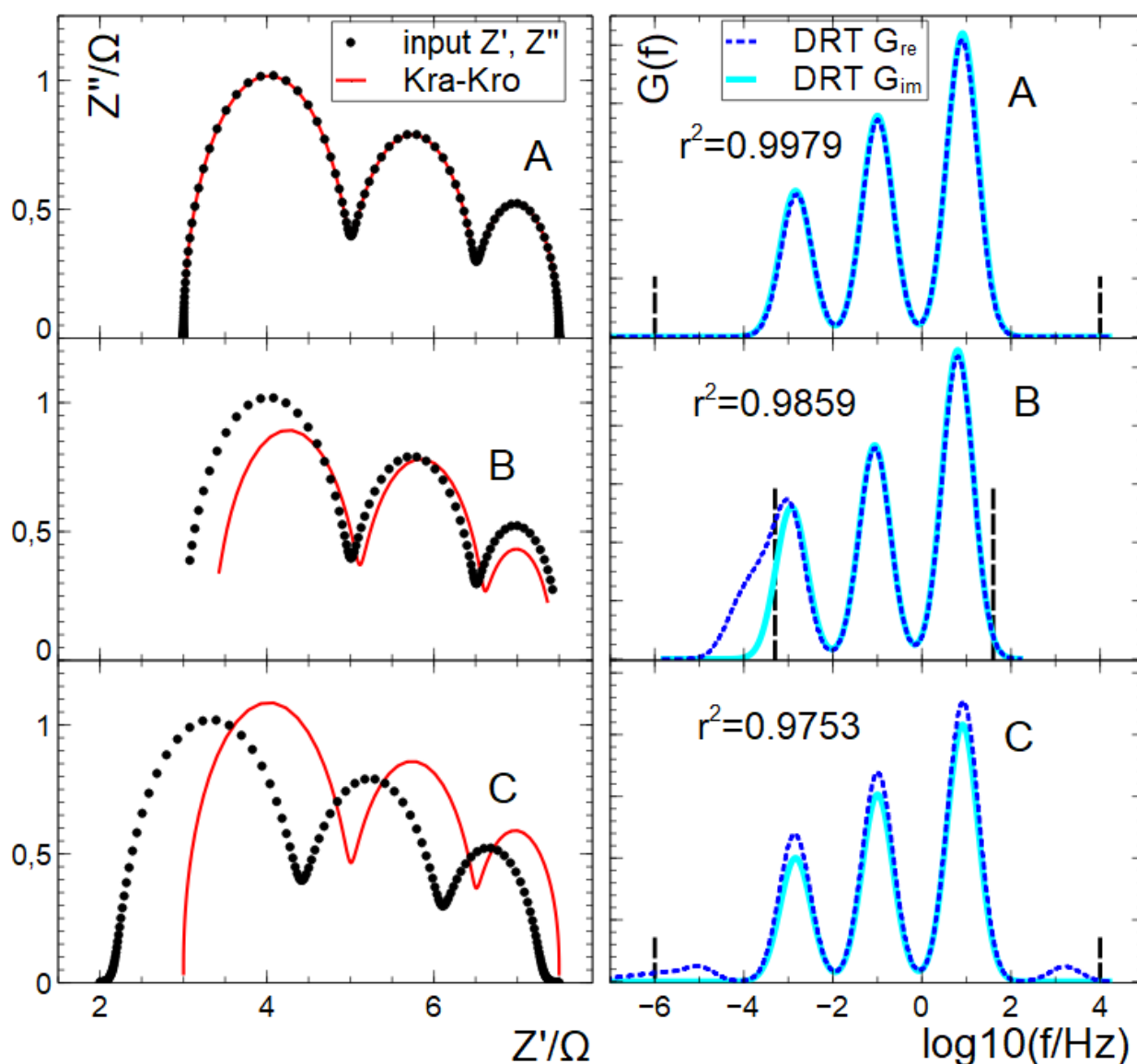


Fig 2: left-hand side: Nyquist plot  $Z''$  vs  $Z'$  of impedance data simulated from a circuit of 3 R-C elements in series (see Fig. 1); red line: Kramers Kronig curve according to Eq. 1

A: reference data, frequency range covers the semi-circles completely

B: as A but some data at lowest and highest frequencies were removed

C: as A but a frequency-dependent drift of  $Z'$  was added (see Fig.1 for details)

Right-hand side: DRT data calculated with DRTtools, from the same data samples A, B, C; with  $G_{Re}$  in dotted dark blue and  $G_{Im}$  in solid light blue; vertical broken lines indicate frequency limits of input data. Note that high frequencies correspond to low resistance

The parameter  $r^2$  was calculated according to Eq. 4, using only data within frequency limits of input.

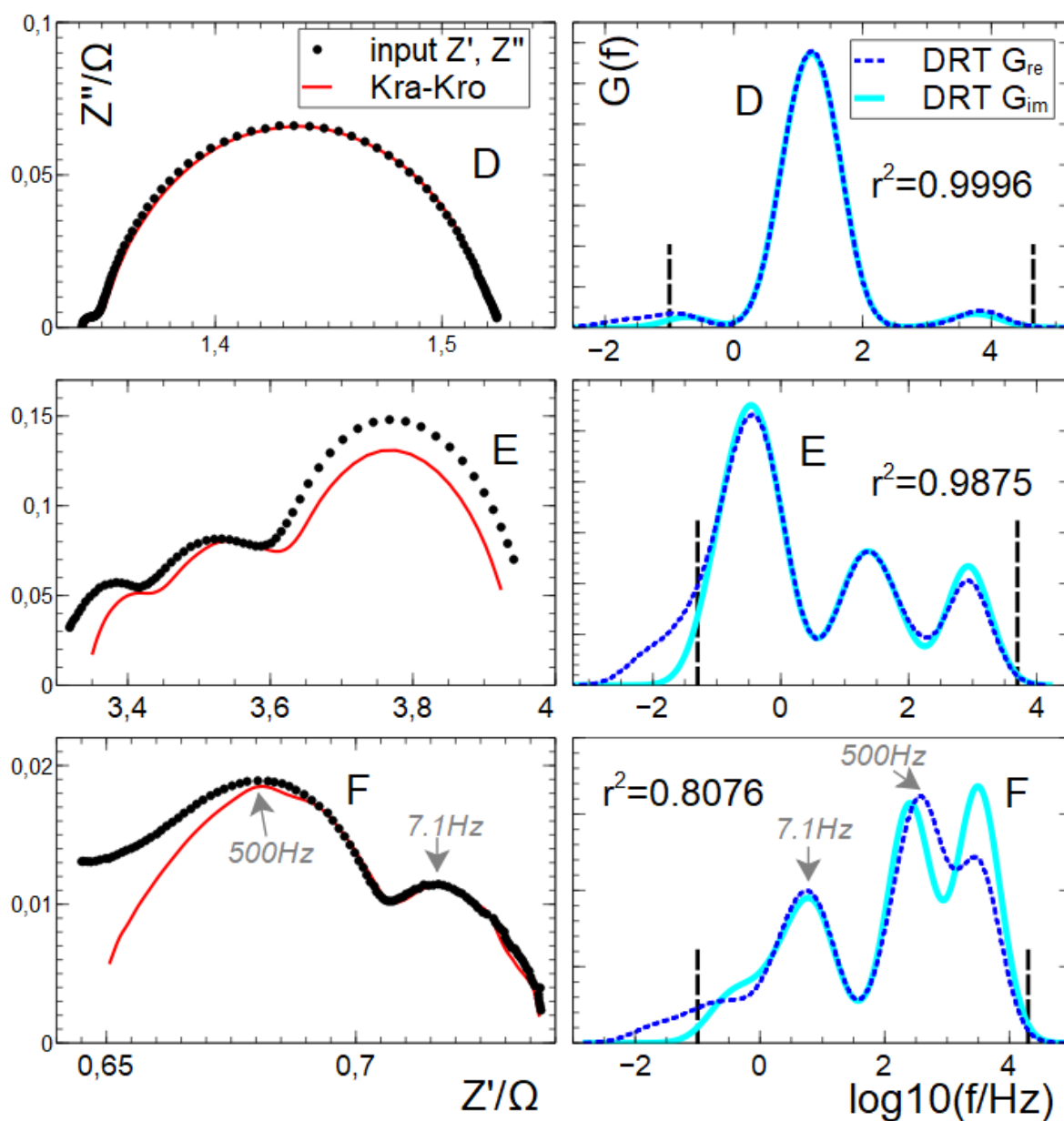


Fig. 3 Left-hand side: Nyquist plot  $Z'$  vs  $Z''$  of three SOFC half cells; black circles: measured data, red lines: Kramers Kronig curve according to Eq. 1 Right-hand side: DRT data calculated with DRTtools, from the same data samples D, E, F; with  $G_{Re}$  in dotted dark blue and  $G_{Im}$  in solid light blue; vertical broken lines indicate frequency limits of input data. The parameter  $r^2$  was calculated according to Eq. 4, using only data within frequency limits of input. In the third row (example F), the frequency values corresponding to the main peaks are indicated for guidance.

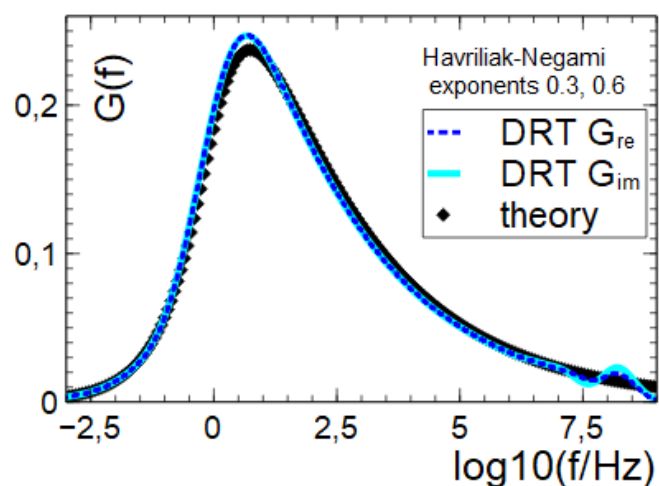


Fig 4: DRT of a Havriliak Negami distribution with exponents 0.3 and 0.6, black diamonds : theoretical curve; blue lines: calculated  $G_{re}$  and  $G_{im}$  from DRTtools using the parameters listed in the text; all curves were rescaled so that their integral equals 1

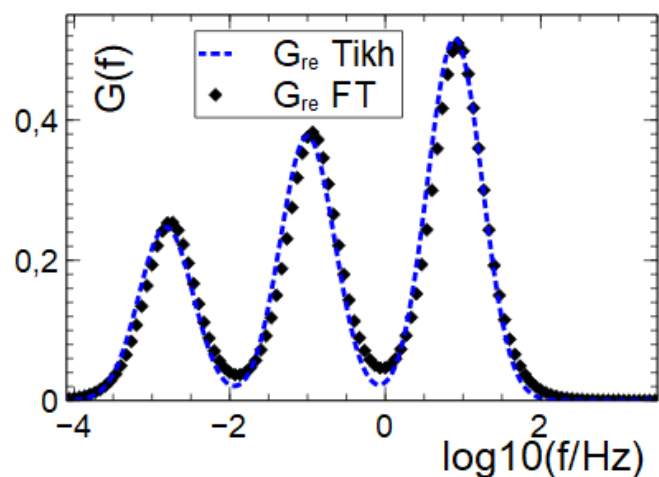


Fig 5: comparison of DRT calculations from Fourier-transformation of a convolution equation (in black diamonds) and from DRTtools (blue dotted line), using  $Z'$  data and the parameters listed in the text. Both curves were rescaled so that their integral is equal to 1, but no filters were applied.